ISSN 2616-5767 Vol.9, Issue 2: 74-80, DOI: 10.25236/AJETS.2026.090210

Microfluidic-based Technology for Fabricating Tumor Invasion Chips

Zeyao Li[1,a,*]

[1]*School of Optical-Electrical and Computer Engineering, University of Shanghai for Science and Technology, Shanghai, 200093, China*
[a] *1321331241@qq.com*
[*]*Corresponding author*

Abstract: *Tumor invasion and metastasis represent major causes of treatment failure and patient mortality in oncology. Three-dimensional tumor spheroid models offer a more physiologically relevant system for mimicking the microstructure and biological behavior of solid tumors. Thus, developing a platform capable of dynamically monitoring spheroid invasion is of significant importance for elucidating metastatic mechanisms and accelerating anti-cancer drug discovery. However, conventional invasion models are often inadequate for real-time, dynamic observation and quantitative analysis, while existing microfluidic models still exhibit limitations in studying three-dimensional tumor invasion. To address these challenges, this study developed a tumor invasion chip based on microfluidic technology, which integrates three-dimensional tumor spheroid culture with chemokine concentration gradient generation. This platform enabled dynamic monitoring of tumor spheroid invasion over a 48-hour period. The results revealed distinct invasion patterns among breast cancer cell lines with varying invasive capacities and demonstrated that epidermal growth factor (EGF) promotes spheroid invasion in a dose-dependent manner. This chip provides a novel technical approach and experimental platform for investigating the mechanisms of cancer cell metastasis.*

Keywords: *Microfluidic chips; chemotactic invasion; 3D cancer spheroid culture*

1. Introduction

According to the 2021 statistics from the World Health Organization (WHO), nearly 10 million people died from cancer in 2020, and it is projected that there will be 28.4 million new cancer cases in 2040[1]. Breast cancer represents one of the most prevalent malignancies among women worldwide, rendering its early diagnosis, therapeutic intervention, and drug efficacy screening central priorities in biomedical research. Conventional clinical management typically involves surgical resection, radiotherapy, chemotherapy, and targeted therapies. However, despite substantial advancements in early detection and therapeutic strategies, tumor metastasis persists as the primary clinical bottleneck[2]. The metastatic process involves a multi-step cascade, including local invasion, intravasation into the circulatory system, survival within the vasculature, extravasation, and colonization at distant organs (e.g., bone[3], lungs[4], liver[5] and[6] brain). This complex progression is tightly orchestrated by dynamic interactions between tumor cells and the tumor microenvironment (TME)[7], encompassing mechanisms such as epithelial-mesenchymal transition (EMT)[8], angiogenesis, immune evasion, and metabolic reprogramming. Consequently, early diagnosis and dynamic monitoring of metastatic breast cancer are imperative for improving patient survival[9]. Despite continuous advancements in medical technologies, the real-time monitoring of cellular migration and metastasis remains a significant research hotspot and a formidable challenge. Specifically, effectively and accurately capturing the dynamic alterations of breast cancer cell migration and invasion during preclinical studies and pharmacological evaluations continues to be a pressing issue to be addressed.

In 2022, the U.S. Senate passed the FDA Modernization Act 2.0, which eliminated the federal mandate for animal testing in the evaluation of new and generic drugs, aiming to significantly reduce the reliance on animal models in the coming years[10]. With the convergence of microfluidic and organoid technologies, organ-on-a-chip (OoC) platforms have emerged as a premier alternative to traditional animal testing[11]. While microfluidic migration assays have made notable strides, conventional chips predominantly focus on single-cell migration, leaving the invasive behaviors of 3D tumor spheroids largely underexplored. To address this, Hockemeyer et al. developed a microfluidic

ISSN 2616-5767 Vol.9, Issue 2: 74-80, DOI: 10.25236/AJETS.2026.090210

device for imaging the interactions between stromal cells and tumor spheroids within a three-dimensional (3D) microenvironment, while enabling external control over interstitial flow at an endothelial cell-supporting interface[12]. Similarly, Lin et al. established an integrated 3D microfluidic platform to mimic the glioma microenvironment[13]. By achieving spatial separation via compartmentalized structures and hydrogels, this platform enables the independent monitoring of cellular morphological alterations and migration, as well as the crosstalk among different cell types. In another notable study, Lee et al. developed a channel-assembled tumor-on-a-chip (CATOC) system[14]. The microfluidic device comprises two distinct channels, allowing for the independent construction and maturation of the vascular and tumor microenvironments prior to their fluidic interconnection. This assembled CATOC platform was successfully utilized to validate the responses of chemotherapeutic and targeted anti-cancer drugs across different breast cancer subtypes within a physiologically relevant TME.

In this study, we engineered a three-dimensional (3D) tumor spheroid invasion chip based on microfluidic technology. Through a combination of theoretical analysis, computational simulations, and experimental validation, we demonstrated the platform's capability to achieve precise spatial patterning of hydrogels and generate stable chemoattractant concentration gradients. Integrating cell assays with live-cell imaging techniques, we systematically investigated the epidermal growth factor (EGF)-regulated invasion behaviors of tumor spheroids derived from two breast cancer cell lines (MDA-MB-231 and MCF-7). Quantitative analysis of the experimental data was performed using ImageJ software. Our findings reveal that MDA-MB-231 and MCF-7 spheroids exhibit distinct, cell-type-specific invasion patterns, with MDA-MB-231 spheroids demonstrating a robust dose-dependent response to varying EGF concentrations. Ultimately, this study provides a novel technical platform for exploring the mechanisms underlying 3D tumor spheroid invasion patterns.

2. Experimental section

2.1 Simulation of hydrogel patterning and concentration gradient

To mimic the human extracellular matrix (ECM), Matrigel was employed as a substitute. The precise spatial patterning of the hydrogel precursor solution within the chip—achieved via the capillary pinning effect without leakage into adjacent channels—was validated using the Two-Phase Flow, Level Set interface in COMSOL Multiphysics software[15]. By defining hydrophobic boundary conditions with a contact angle of 120°, parameters including the dynamic viscosity, density, and surface tension of the hydrogel were configured. A transient solver was subsequently utilized for the computation, and the simulation results are presented in Fig. 1(a). The hydrogel successfully exhibited capillary pinning in the designated channel; constrained by surface tension, it was anchored between the micropillars and remained stable without leaking into adjacent compartments.

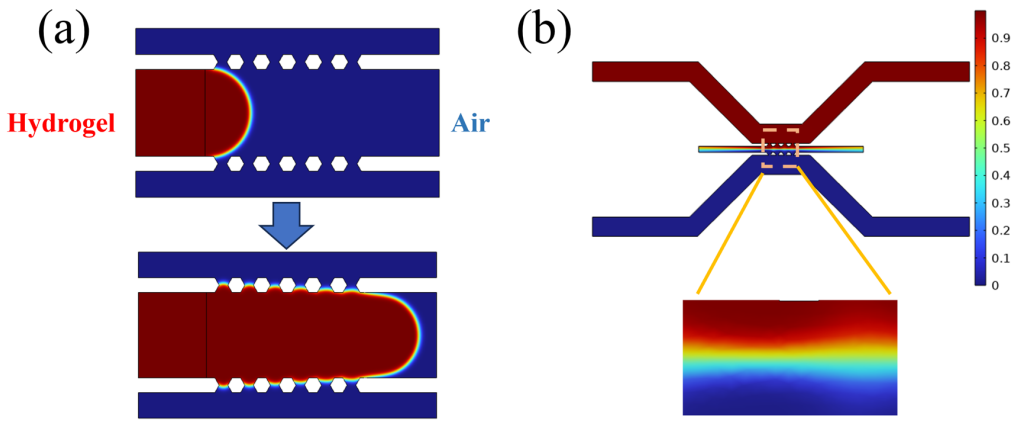

Fig. 1 Comsol simulation. (a) Simulation of Hydrogel Patterning; (b) Simulation of Concentration Gradient Generation.

In vivo, the distant metastasis of tumor cells is not a random event but is precisely guided by complex chemical signaling networks. Chemoattractants, such as epidermal growth factor (EGF) and

ISSN 2616-5767 Vol.9, Issue 2: 74-80, DOI: 10.25236/AJETS.2026.090210

stromal cell-derived factor-1α (SDF-1α), secreted by specific tissues or tumor stromal cells, form concentration gradients within the interstitium, providing a "navigation path" for cancer cells expressing corresponding receptors. Therefore, reconstructing this stable and controllable gradient signal on-chip is fundamental to ensuring the physiological relevance of the in vitro model. In this study, COMSOL Multiphysics was utilized to couple the Laminar Flow and Transport of Diluted Species interfaces, defining the entire fluidic domain as the culture medium. Boundary conditions were established by normalizing the concentration at the chemoattractant loading inlet to 1 mol/m³, while the other inlet, designated for the culture medium, was set to 0 mol/m³. Finally, the model was solved under steady-state conditions. As depicted in Fig. 1(b), a stable chemotactic gradient was formed under steady state, presenting a distinct concentration boundary within the central region.

2.2 Design and fabrication of the microfluidic chip

The microfluidic device architecture was designed using SolidWorks software. The chip comprises three parallel microchannels for introducing distinct reagents, with adjacent channels separated by micropillars and a uniform channel height of 160 μm. The completed design was then transferred onto a photomask. Subsequently, an SU-8 master mold was fabricated on a 4-inch silicon wafer via standard soft lithography techniques, as illustrated in Fig. 2(a-b).

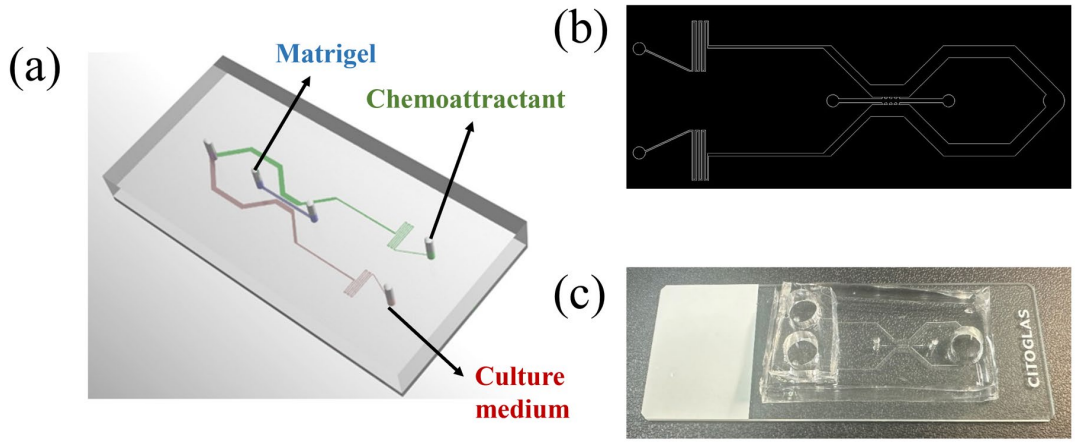

Fig. 2 Design and Photograph of the Chip. (a) Schematic diagram of the microfluidic chip; (b) Photomask of the microfluidic chip; (c) Photograph of the microfluidic chip.

SU-8 is an epoxy-based negative photoresist widely utilized for its reliable quality, excellent optical transparency, and high chemical stability. Following plasma cleaning of the bare silicon wafer, the SU-8 photoresist was applied and subjected to a sequential fabrication protocol: spin-coating, soft baking, UV exposure, post-exposure baking (PEB), development, and hard baking, as delineated in Fig. 3. The topological height and structural integrity of the microchannels were subsequently verified using a surface profilometer. Upon completion of the silicon master mold, polydimethylsiloxane (PDMS) prepolymer and its curing agent were mixed at a 10:1 (w/w) ratio, thoroughly degassed under vacuum, and thermally cured in an oven at 80°C for 1.5 h. The solidified PDMS replica was then peeled off the mold and irreversibly bonded to a glass slide via oxygen plasma activation. A photograph of the fully assembled device is depicted in Fig. 2(c). To restore the inherent surface hydrophobicity—a crucial prerequisite for precise hydrogel patterning—the bonded chip was baked overnight at 80°C. Finally, the device was sterilized via ultraviolet (UV) irradiation prior to use.

ISSN 2616-5767 Vol.9, Issue 2: 74-80, DOI: 10.25236/AJETS.2026.090210

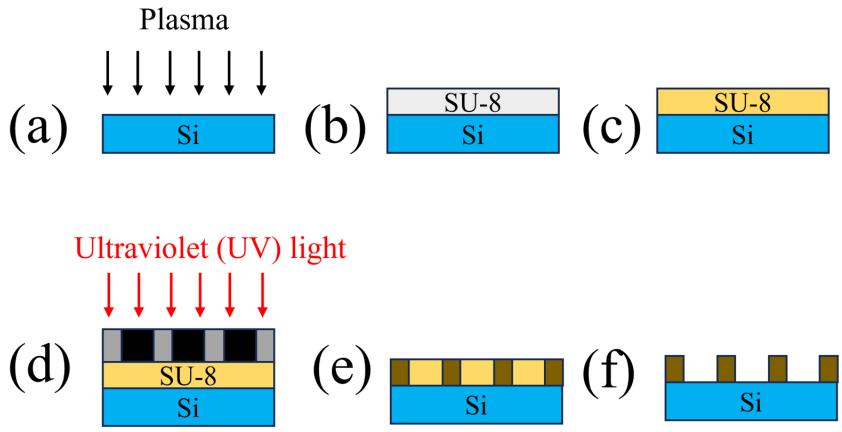

Fig. 3 Schematic of the Photolithography Process. (a) Plasma cleaning; (b) Dispensing, Spin-coating; (c) Soft Bake; (d) Exposure; (e) Post-Exposure Bake; (f) Development.

2.3 Cell culture and reagent preparation

Human breast cancer cell lines MDA-MB-231 and MCF-7 were cultured in DMEM/F-12 medium (01-172-1ACS, BI) supplemented with 10% (v/v) fetal bovine serum, 1% penicillin, and 1% streptomycin. The cells were seeded in T25 culture flasks and maintained in a humidified incubator at 37°C with a 5% CO_2 atmosphere. Upon reaching 70%–90% confluence, the cells were detached via trypsinization, resuspended, and subcultured. The chemoattractant epidermal growth factor (EGF; AF-100-15-500, PeproTech) was aliquoted according to the manufacturer's instructions and subsequently diluted to final working concentrations of 0.25, 2.5, and 8.33 nM. To characterize the generation of an appropriate concentration gradient, FITC-dextran (10 kDa; FD-10S; Sigma, Oakville, Canada) was supplemented into the chemoattractant solution. Matrigel (356234, Corning) was mixed with the culture medium at a volume ratio of 1.5:1. Finally, a Calcein/PI assay (C2015 M, Beyotime) was utilized for live/dead cell staining.

2.4 Tumor spheroid generation and on-chip invasion assay

Tumor spheroids were generated utilizing the standard hanging drop method, allowing a 24-hour incubation period for the cells to aggregate and form compact spheroids. Representative bright-field images of the fully formed MDA-MB-231 and MCF-7 breast cancer spheroids are presented in Fig. 4(a-b). The mature spheroids were harvested and centrifuged for 30 s. Subsequently, they were resuspended in the pre-prepared Matrigel and culture medium mixture. Using a micropipette, the spheroid suspension was gently loaded into the central channel of the microfluidic chip. All aforementioned procedures were strictly performed on ice to prevent premature gelation of the Matrigel.

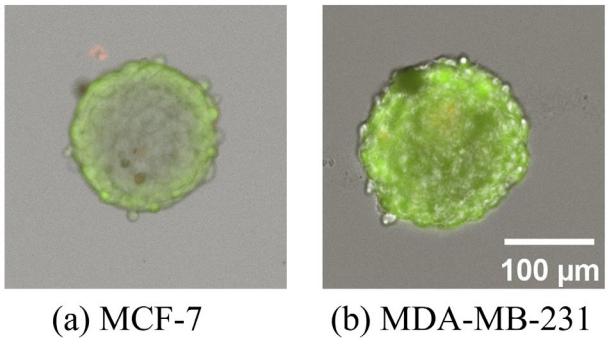

Fig. 4 Morphology and viability of hanging drop-generated tumor spheroids at 24 h.

Upon successful loading of the spheroid-laden Matrigel solution into the device, the chip was incubated at 37 °C for 30 min to allow for thermal gelation. Following polymerization, the

ISSN 2616-5767 Vol.9, Issue 2: 74-80, DOI: 10.25236/AJETS.2026.090210

chemoattractant and culture medium were introduced into the respective lateral channels. The invasive behavior of the tumor spheroids was monitored and recorded over a 48 h period, with the media and chemoattractant being replenished at 12 h intervals.

3. Results and Discussion

3.1 Validation of hydrogel patterning and concentration gradient generation

Guided by the aforementioned theoretical analysis and COMSOL simulation results, the structural parameters of the microfluidic device were established. To verify the reliability of the hydrogel patterning process and concentration gradient generation, the Matrigel-medium mixture was injected into the central channel using a micropipette. Concurrently, culture medium containing FITC-dextran and plain culture medium were loaded into the respective side channels. The device was then placed under a fluorescence microscope to monitor gradient formation in the central channel, with the experimental results shown in Fig. 5(a-b). During the hydrogel patterning phase, bright-field microscopy revealed a distinct capillary pinning effect between the micropillars. This effect effectively confined the hydrogel within the central channel, preventing any lateral leakage into the adjacent compartments. Furthermore, quantitative grayscale analysis of the FITC-dextran fluorescence distribution confirmed that a stable concentration gradient was successfully established within the central channel.

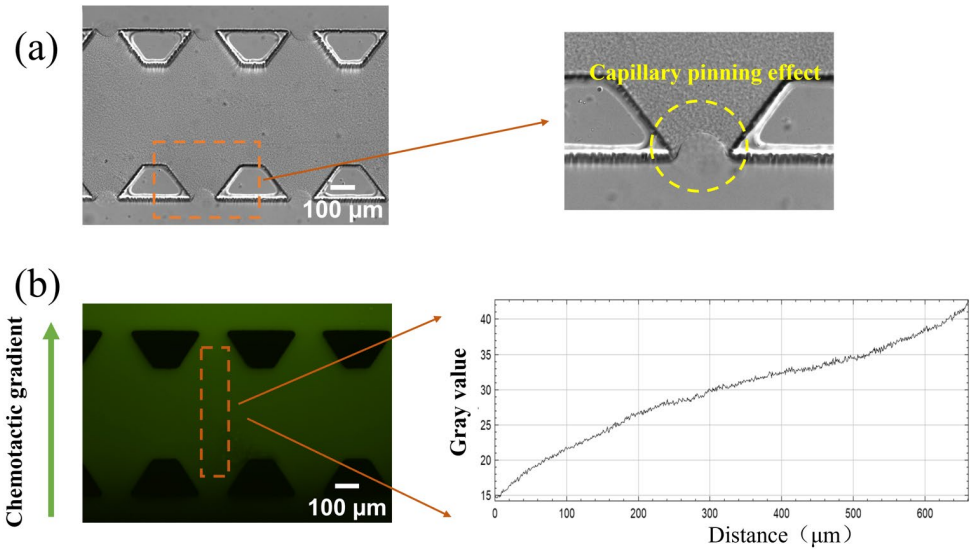

Fig. 5 Microscopic Concentration Gradient Generation and Hydrogel Patterning. (a) Bright-field image of the patterned hydrogel; (b) Fluorescence characterization of the concentration gradient.

3.2 Differential invasion patterns of distinct breast cancer cell lines in a 3D matrix

The EGF-induced invasion of MDA-MB-231 and MCF-7 spheroids was monitored at 24 h intervals via bright-field microscopy, revealing that the two cell lines exhibited distinctly different invasion patterns within the 3D matrix. As shown in Fig. 6(a), MCF-7 spheroids maintained their overall structural integrity and advanced outward primarily via collective migration. The cell spheroids formed a continuous migratory front, achieving coordinated collective movement. In contrast, MDA-MB-231 spheroids displayed a mesenchymal-like single-cell invasion pattern, where individual cells actively detached from the spheroid core and migrated radially into the surrounding matrix, as depicted in Fig. 6(b).The differential invasion patterns of these two cell lines are highly consistent with their respective molecular subtypes[16]. The single-cell invasion mode exhibited by MDA-MB-231 spheroids aligns with their mesenchymal phenotype and low E-cadherin expression; this profile facilitates protease-dependent matrix remodeling and independent cell motility. Conversely, the collective invasion behavior of MCF-7 spheroids corresponds to their epithelial characteristics and high E-cadherin expression, wherein strong cell-cell adhesion inhibits the detachment of individual cells, thereby sustaining the coordinated migration of the population.

ISSN 2616-5767 Vol.9, Issue 2: 74-80, DOI: 10.25236/AJETS.2026.090210

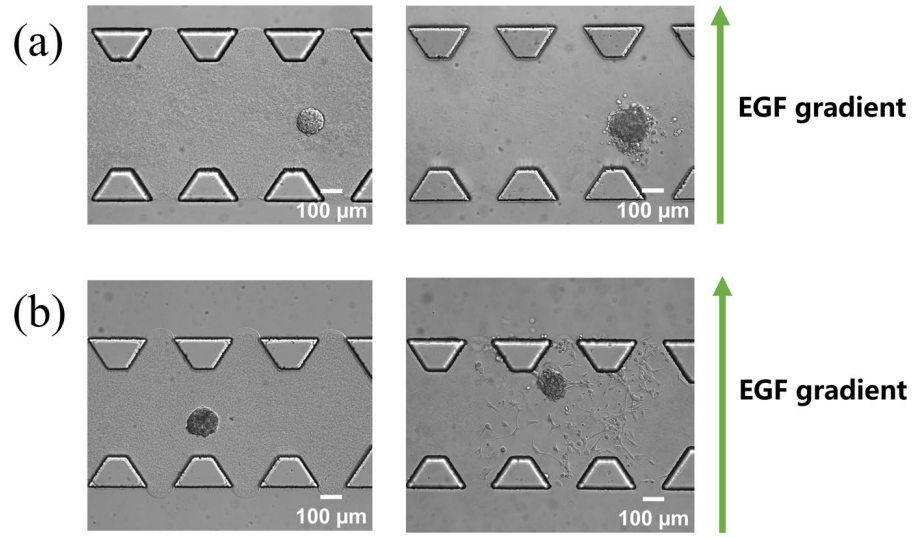

Fig. 6 Bright-field images of MCF-7 and MDA-MB-231 spheroids after 48-hour invasion under an EGF gradient. (a) Invasion of MCF-7 spheroids after 48 h of incubation; (b) Invasion of MDA-MB-231 spheroids after 48 h of incubation

3.3 EGF promotes MDA-MB-231 spheroid invasion in a dose-dependent manner

To investigate the impact of EGF concentration on the invasive capacity of breast cancer spheroids, MDA-MB-231 cells — characterized by their mesenchymal migration and single-cell invasive phenotype—were selected as the model for quantitative invasion analysis. The results demonstrated that under stimulation with varying concentrations of EGF, the number of cells migrating outward from the spheroids significantly increased compared to the control group, exhibiting a pronounced dose-dependent enhancement (Fig. 7). Specifically, the number of disseminating cells in the 8.33 nM EGF-treated group was approximately 3.6-fold higher than that of the control group, representing a 1.93-fold increase relative to the 0.25 nM EGF group.

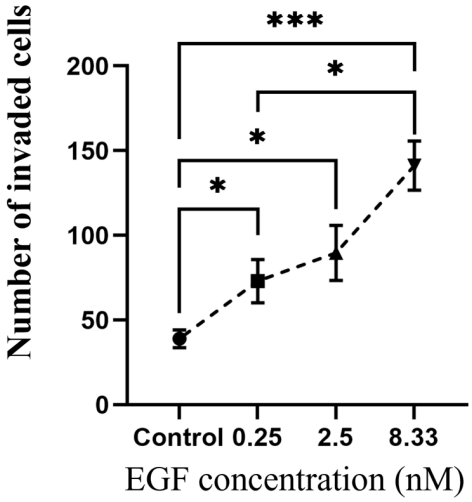

Fig. 7 Quantitative Analysis of MDA-MB-231 Spheroid Invasion under EGF Gradients at 48 h

4. Conclusion

In this study, we successfully fabricated a microfluidic chip utilizing soft lithography, specifically designed for the dynamic monitoring of tumor spheroid invasion behaviors. The feasibility of on-chip hydrogel patterning and chemoattractant gradient formation was theoretically and empirically validated

ISSN 2616-5767 Vol.9, Issue 2: 74-80, DOI: 10.25236/AJETS.2026.090210

through COMSOL simulations, demonstrating the platform's exceptional flexibility to accommodate diverse reagents and tumor spheroid models. In contrast to conventional microfluidic systems that primarily focus on 2D cell migration or 3D single-cell invasion, our study successfully reconstructed a highly physiologically relevant 3D collective invasion model—closely mimicking the authentic in vivo microenvironment—by co-embedding tumor spheroids within a Matrigel matrix.

Utilizing this platform, we comparatively analyzed the invasive behaviors of different breast cancer cell lines (MDA-MB-231 and MCF-7), successfully observing characteristic invasion patterns that perfectly align with their respective molecular subtypes. Furthermore, our findings demonstrated that EGF significantly promotes spheroid invasion in a distinct dose-dependent manner. Compared to existing technologies, our microfluidic device offers several key advantages: high adaptability to various cell lines and reagents, the capability for real-time dynamic tracking of the invasion process, and significantly minimized consumption of valuable cells and reagents. Ultimately, this tumor invasion chip provides a robust and versatile research platform for the future development of complex organ-on-a-chip models and the in-depth exploration of cancer invasion and metastasis mechanisms.

References

[1] Tian Y., Kang W. New progress in research on global cancer incidence[J]. China Medicine, 2021, 16(10): 1446-1447.

[2] Tang D D, Ye Z J, Liu W W, et al. Survival feature and trend of female breast cancer: A comprehensive review of survival analysis from cancer registration data[J]. Breast, 2025, 79.

[3] Zhu M Y, Liu X, Qu Y, et al. Bone metastasis pattern of cancer patients with bone metastasis but no visceral metastasis[J]. Journal of Bone Oncology, 2019, 15.

[4] Edwards C M, Johnson R W. Targeting Histone Modifications in Bone and Lung Metastatic Cancers[J]. Current Osteoporosis Reports, 2021, 19(3): 230-246.

[5] Andryszkiewicz W, Misiag P, Karwowska A, et al. Cancer Metastases to the Liver: Mechanisms of Tumor Cell Colonization[J]. Pharmaceuticals, 2024, 17(9).

[6] Chen W W, Chu T S M, Xu L L, et al. Immune related biomarkers for cancer metastasis to the brain[J]. Experimental Hematology & Oncology, 2022, 11(1).

[7] Xiao Y H, Hassani M, Moghaddam M B, et al. Contribution of tumor microenvironment (TME) to tumor apoptosis, angiogenesis, metastasis, and drug resistance[J]. Medical Oncology, 2025, 42(4).

[8] Rhim A D, Mirek E T, Aiello N M, et al. EMT and Dissemination Precede Pancreatic Tumor Formation[J]. Cell, 2012.

[9] Trayes K P, Cokenakes S E H. Breast Cancer Treatment[J]. American Family Physician, 2021, 104(2): 171-78.

[10] Stresser D M, Kopec A K, Hewitt P, et al. Towards in vitro models for reducing or replacing the use of animals in drug testing[J]. Nature Biomedical Engineering, 2024, 8(8): 930-935.

[11] Lacombe J, Dunn S E, Layac M, et al. A human 3D culture-organ-on-chip platform for investigating the tumor microenvironment response[J]. Iscience, 2026, 29(1).

[12] Hockemeyer K, Janetopoulos C, Terekhov A, et al. Engineered three-dimensional microfluidic device for interrogating cell-cell interactions in the tumor microenvironment[J]. Biomicrofluidics, 2014, 8(4): 12.

[13] Lin L, He Z Y, Jie M S, et al. 3D microfluidic tumor models for biomimetic engineering of glioma niche and detection of cell morphology, migration and phenotype change[J]. Talanta, 2021, 234: 5.

[14] Lee J, Kim Y, Jung H I, et al. Channel-assembling tumor microenvironment on-chip for evaluating anticancer drug efficacy[J]. J Control Release, 2025, 377: 376-384.

[15] Nguyen T T Y, Lee J, Choi S, et al. Surface Tension-Based Open Microfluidic Platform Using Micropillars to Recreate the 3D Lung Cellular Microenvironment[J]. Biochip Journal, 2024, 18(4): 589-600.

[16] Chen S Q, Qi H, Kuang Y H, et al. Monitoring the mechanical responses of tumor metastasis based on a microfluidic chip integrated with an electrochemical detection system[J]. Lab Chip, 2025, 25(15): 3858-3867.